

Bit Efficient Toeplitz Covariance Estimation

Hongwei Xu, Zai Yang, *Senior Member, IEEE*

Abstract—This paper addresses the challenge of Toeplitz covariance matrix estimation from partial entries of random quantized samples. To balance trade-offs among the number of samples, the number of entries observed per sample, and the data resolution, we propose a ruler-based quantized Toeplitz covariance estimator. We derive non-asymptotic error bounds and analyze the convergence rates of the proposed estimator. Our results show that the estimator is near-optimal and imply that reducing data resolution within a certain range has a limited impact on the estimation accuracy. Numerical experiments are provided that validate our theoretical findings and show effectiveness of the proposed estimator.

Index Terms—Quantization, dithering, covariance estimation, Toeplitz covariance matrix.

I. INTRODUCTION

ESTIMATING the covariance matrix of a distribution \mathcal{D} based on independent random vectors $\mathbf{x}^{(1)}, \dots, \mathbf{x}^{(n)} \sim \mathcal{D}$ is a fundamental problem in statistics. This problem is particularly prominent in applications such as signal processing [1] and pattern recognition [2], where accurate covariance estimation plays a crucial role. Over the years, significant attention has been devoted to this challenge, resulting in numerous advancements, as evidenced by recent works such as [3, 4].

In covariance estimation problems, it is often assumed that the covariance matrix T is a *symmetric Toeplitz matrix*, i.e., it satisfies $T_{a,b} = T_{c,d}$ whenever $|a - b| = |c - d|$. This assumption naturally arises in stationary processes, where the covariance between measurements at two points depends only on the distance between them. The Toeplitz structure is particularly prevalent in applications such as direction-of-arrival (DOA) estimation [5], radar image processing [6], and other related programs.

For the Toeplitz covariance estimation problem, the goal is to approximate T using as few bits of sample information as possible. This objective is motivated by the need to reduce the amount of information that must be acquired or transmitted. Unlike general covariance estimation, the focus here is on the estimator that leverage only a subset of the entries from each quantized coarse sample $\hat{\mathbf{x}}^{(l)}$. Here, the quantization process maps the exact values of the samples to a discrete form, see Fig. 2 in the main context.

When considering the number of bits required for the estimator \hat{T} to achieve a given tolerance ϵ , i.e.,

$$\|T - \hat{T}\|_2 \leq \epsilon \|T\|_2, \quad (1)$$

the following aspects are typically of interest:

- **Vector Sample Complexity (VSC):** The number of coarse samples $\hat{\mathbf{x}}^{(1)}, \dots, \hat{\mathbf{x}}^{(n)}$ required by the estimator \hat{T} to approximate T .
- **Entry Sample Complexity (ESC):** The number of entries observed in each coarse sample.
- **Resolution:** Higher resolution is achieved with more precise entries, while lower resolution results from less accurate samples. It is typically determined by the quantization level Δ , where a larger Δ corresponds to lower resolution.

The goal of achieving a covariance estimation that meets the requirement (1) necessitates a trade-off among these three factors, as simultaneously minimizing all three is typically infeasible.

The trade-off between VSC and ESC have been extensively analyzed in [7], albeit without considering resolution. The results demonstrate that, even with a relatively small ESC, (1) can still be achieved by increasing the number of observed samples (i.e., VSC). On the contrary, in general covariance estimation settings, studies have shown that quantization, while reducing resolution, only slightly worsens the leading factors of the estimation error and does not affect the scaling order [8, 9].

However, to the best of the authors' knowledge, no existing studies simultaneously consider the three factors of VSC, ESC, and resolution. The aim of this paper is to propose a novel estimator \hat{T} that enables a reasonable trade-off among these three factors, thus advancing the understanding of covariance estimation in Toeplitz settings.

A. Relations to Prior Art

Estimating the covariance matrix by acquiring all the entries of each sample has been a significant topic in statistics [10]. Classical methods, such as maximum likelihood estimation [11] and projected covariance estimation [12], have been extensively studied. In addition, methods that consider only a subset of the entries in each sample has also been explored [13]. The introduction of the Toeplitz property into these methods has been shown to significantly enhance estimation performance [14]. This improvement arises from the inherent translational invariance of the covariance matrix in stationary processes, which effectively reduces the degrees of freedom required for estimation in practical applications [15]. Leveraging the Toeplitz property not only improves estimation accuracy but also reduces computational complexity.

To address the Toeplitz covariance estimation problem, sparse recovery methods built on the Vandermonde decomposition of T have been employed [13, 16]. In particular, several well-known algorithms, such as MUSIC and ESPRIT methods, have been studied under the low-rank setting. Furthermore,

The authors are with the School of Mathematics and Statistics, Xi'an Jiaotong University, Xi'an 710049, China (e-mails: bracy.xu@gmail.com, yangzai@xjtu.edu.cn).

under the strong separation assumption, sparse Fourier transform methods can be applied to solve this problem [7, 17]. Exploiting the structural properties of the Toeplitz covariance matrix, it is often sufficient to consider only a subset of entries from each sample. The indices of this subset are referred to as the *ruler* (see Definition 1), which is analogous to the sparse array in array signal processing. Consequently, the trade-off between VSC and ESC becomes a critical consideration. To address this, numerous studies have explored sparse ruler-based methods, which have found widespread applications in signal processing [18, 19].

Some results have been established for the ruler-based estimator \hat{T} . Preliminary analyses of the estimation error $\|T - \hat{T}\|_2$ are presented in [20]. Further advancements, including non-asymptotic bounds in the sense of the Frobenius norm, have been provided in [21]. More recently, non-asymptotic bounds in terms of operator norm have been established in [22], further refining the estimation error analysis in Toeplitz matrix recovery. Groundbreaking results were achieved in [7], where the relationship between ESC and VSC was comprehensively analyzed in different cases, leading to more general conclusions.

Besides covariance estimation, our research is also related to quantization. Quantization plays a critical role in reducing the resolution of data, which is crucial for reducing the cost of data processing [8]. For instance, in multiple-input multiple-output (MIMO) communication systems, the frequent transmission of high-resolution data imposes significant processing costs. By quantizing the transmitted data to lower resolutions, these costs can be substantially reduced [23]. Motivated by practical needs, quantization theory has been extensively explored, including 1-bit quantization [24–27] and multi-bits quantization [8, 28, 29].

Quantization refers to the process of mapping continuous inputs to discrete form [30]. Various quantization approaches have been proposed to address different problem domains. For example, [24] introduces two methods for 1-bit quantization, which map continuous signals to ± 1 . The first method, dither-free quantization, directly maps data x to $\text{sign}(x)$, while the second method, dithered quantization, involves adding a uniform dither to the data before quantization. In addition, [8] considers a multi-bits dithered quantization approach and analyzes the properties of both uniform and triangular dithers. Notably, these quantization techniques are memoryless, meaning that the quantization of each data is independent to the others. In addition to these methods, other quantization approaches have also been studied [31]. The choice of quantization method often depends on the specific problem to be addressed, with different techniques tailored to achieve optimal results in various scenarios.

Research on quantized covariance estimation remains relatively limited. The problem of 1-bit quantized covariance estimation is explored in [24], where non-asymptotic bounds on the operator norm are analyzed. These results are shown to effectively address sparse covariance matrices, providing a valuable framework for handling such cases. This line of work is further extended in [3]. Multi-bits quantized covariance estimation is investigated in [8], particularly for data with

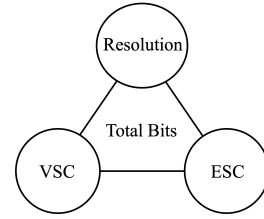


Fig. 1: The “Impossible Triangle” in Toeplitz covariance estimation: for a given tolerance ϵ , to achieve $\|T - \hat{T}\|_2 \leq \epsilon\|T\|_2$, it is impossible to simultaneously minimize VSC, ESC and resolution

heavy-tailed distributions. The study derives non-asymptotic bounds of the error on the operator norm and demonstrates that the proposed method achieves near-optimality. These findings highlight the effectiveness of multi-bit quantization techniques in addressing the challenges posed by heavy-tailed distributions, further enriching the theoretical landscape of quantized covariance estimation.

B. Our Contributions

Distinguishing our study from existing research, we focus specifically on quantized Toeplitz covariance estimation. The primary contribution of this work is the proposal of a novel estimator that facilitates trade-offs among VSC, ESC and resolution. Furthermore, we establish non-asymptotic bounds for the proposed estimator, providing theoretical guarantees for its performance. This work not only extends the existing literature on (quantized) covariance estimation but also introduces new insights into the interplay between sample complexity and quantization resolution.

1) *Realized trade-offs between VSC, ESC, and resolution.* We propose an estimator \hat{T} , modified from the ruler-based estimator, that achieves a balanced trade-off among VSC, ESC and resolution. Specifically, we demonstrate that to achieve $\|T - \hat{T}\|_2 \leq \epsilon\|T\|_2$, it is impossible to simultaneously minimize VSC, ESC, and resolution (e.g., Fig. 1). Furthermore, our results show that decreasing any one (or two) of these quantities can be compensated by increasing the remaining quantity. We provide an in-depth analysis of the constraints governing these three factors.

2) *Non-asymptotic bounds for the estimator \hat{T} .* We derived non-asymptotic bounds that guarantee the performance of the proposed estimator \hat{T} . Our results demonstrate that even when using quantized coarse sample data and observing only a subset of the entries in each sample, the estimator still achieves good performance. This highlights the effectiveness of \hat{T} and shows that highly accurate covariance estimation can be achieved using only a limited amount of sample information.

3) *Near-optimal convergence rates.* We show that quantization only affects the rate of convergence slightly. Compared to the unquantized results in [7], our convergence rates differ solely in the coefficient. This indicates that reducing the sample resolution within a reasonable range has little impact on the estimation accuracy. Notably, our results degenerate into those in [7] in the case when the data is unquantized.

Our results have significant practical values; offering the potential to substantially reduce data processing costs, and providing valuable insights into the trade-off and efficiencies inherent in quantized Toeplitz covariance estimation.

C. Notations

The set of real numbers is denoted by \mathbb{R} . For a positive integer d , let $[d] = \{0, 1, \dots, d-1\}$. Boldface letters are used to represent vectors, where the j -th entry of a vector \mathbf{x} is denoted by x_j . Matrices are denoted by regular letters, with $A_{j,k}$ representing the (j, k) -th entry of a matrix A . For a matrix A , we consider its trace $\text{tr}(A)$, rank $\text{rank}(A)$, operator (spectral) norm $\|A\|_2$, Frobenius norm $\|A\|_F$, and maximum norm $\|A\|_\infty$.

For any vector $\mathbf{a} = (a_0, \dots, a_{d-1})^T \in \mathbb{R}^d$, let $\text{Toep}(\mathbf{a}) \in \mathbb{R}^{d \times d}$ denote the symmetric Toeplitz matrix with entries $\text{Toep}(\mathbf{a})_{j,k} = a_{|j-k|}$. We denote $\text{avg}(A)$ as the Toeplitz matrix obtained by averaging the diagonals of A . For a matrix $A \in \mathbb{R}^{d \times d}$ and a set $R \subset [d]$, let $T_R \in \mathbb{R}^{|R| \times |R|}$ represent the principal submatrix of A , with rows and columns indexed by R , where $|R|$ is the cardinality of R .

For a random variable X , its expectation is denoted by $\mathbb{E}(X)$. The sub-exponential norm $\|X\|_{\psi_1}$ and sub-Gaussian norm $\|X\|_{\psi_2}$ are defined as

$$\|X\|_{\psi_1} = \inf\{t > 0 : \mathbb{E} \exp(|X|/t) \leq 2\} \quad (2)$$

and

$$\|X\|_{\psi_2} = \inf\{t > 0 : \mathbb{E} \exp(X^2/t^2) \leq 2\}, \quad (3)$$

respectively. For real numbers $a < b$, we write $X \sim \mathcal{U}([a, b])$ if and only if X follows a uniform distribution over the interval $[a, b]$.

D. Organization

The rest of the paper is organized as follows. In Section II, we revisit the preliminaries that will be used throughout the article. Section III formally defines the ruler-based quantized Toeplitz covariance estimation problem and introduces an unbiased estimator. In Section IV, we analyze the non-asymptotic performance of the proposed estimator and further investigate its convergence rate. Section V explores two special cases, i.e., the low-rank and band-limited scenarios. Detailed proofs of the theoretical results are provided in the appendices.

II. PRELIMINARIES

In this section, we introduce the key concepts related to ruler-based Toeplitz covariance estimation and quantization. These concepts serve as foundational knowledge that will be applied in subsequent sections.

A. Ruler-based Toeplitz Covariance Estimation

Traditional covariance estimation addresses the problem of estimating the covariance matrix T from independent and identically distributed (i.i.d.) samples drawn from a d -dimensional normal distribution, where $T \in \mathbb{R}^{d \times d}$ is a positive semidefinite matrix, i.e., $\mathbf{x}^{(1)}, \dots, \mathbf{x}^{(n)} \sim \mathcal{N}(0, T)$, given query access to

the sample entries. The objective is to obtain an estimator \tilde{T} that satisfies, with probability at least $1 - \delta$,

$$\|T - \tilde{T}\|_2 \leq \epsilon \|T\|_2, \quad (4)$$

where $\|\cdot\|_2$ denotes the operator norm.

Moreover, when T is a symmetric Toeplitz matrix, it can be fully characterized by a vector \mathbf{a} , where a_s represents the value on the $(s+1)$ -th diagonal of T . Specifically, a_s corresponds to the covariance of samples separated by s indices. Consequently, it suffices to extract a subset of entries $R \subset [d]$ from each sample $\mathbf{x} \sim \mathcal{N}(0, T)$ for distances $s = 0, \dots, d-1$. This observation implies that covariance estimation can be performed more efficiently under the Toeplitz structure.

In Toeplitz covariance estimation, the goal is to approximate T within a given tolerance ϵ while only observing a subset of entries from each sample and using as few samples as possible. To formalize this approach, the concept of a *ruler* is introduced [7].

Definition 1: A subset $R \subset [d]$ is called a *ruler* if for all $s = 0, \dots, d-1$, there exist $j, k \in R$ such that $|j-k| = s$. We further let R_s denote the set of ordered pairs (j, k) with distance s .

We say R is *sparse* if $|R| < d$. For example, when $d = 10$, a sparse ruler can be $R = \{1, 2, 5, 8, 10\}$. Sparse ruler are also called redundancy sparse arrays or sparse linear arrays in the literature [32]. Note that sparse rulers are not unique. In general, a sparse ruler must satisfy $\sqrt{d} \leq |R| < d$ [33]. For any d , we introduce a type of rulers as follows.

Definition 2: For $\alpha \in [1/2, 1]$, let R_α denote a ruler defined as

$$R_\alpha = R_\alpha^{(1)} \cup R_\alpha^{(2)}, \quad (5)$$

where

$$R_\alpha^{(1)} = \{1, 2, \dots, d^\alpha\} \quad (6)$$

and

$$R_\alpha^{(2)} = \{d, d - d^{1-\alpha}, \dots, d - (d^\alpha - 1)d^{1-\alpha}\}. \quad (7)$$

For simplicity, we assume that both d^α and $d^{1-\alpha}$ are integers. In practical applications, rounding non-integer values to the nearest integer is sufficient. For example, when $d = 16$, the sparse ruler $R_{1/2} = \{1, 2, 3, 4, 8, 12, 16\}$ exemplifies Definition 2. As will be demonstrated in subsequent sections, this type of ruler possesses several desirable properties, making it a compelling choice in scenarios where reducing the number of entries observed in each sample is critical. Notably, when $\alpha = 1$, i.e., $R = [d]$, we refer to it as the *full ruler*, which corresponds to the classic case.

For brevity, we then introduce the concept of the *coverage coefficient* here [7].

Definition 3: For any ruler $R \subset [d]$, the *coverage coefficient* is defined as

$$\phi(R) := \sum_{s=1}^{d-1} \frac{1}{|R_s|}. \quad (8)$$

where R_s is as specified in Definition 1.

As the distance s is represented more frequently in the ruler R , the value of $\phi(R)$ decreases. The coverage coefficient plays

a crucial role in the subsequent proofs. Intuitively, it can be observed that

$$\phi(R_1) = O(\log d), \quad \phi(R_{1/2}) = O(d). \quad (9)$$

A ruler-based Toeplitz covariance estimator can be defined as $\tilde{T} = \text{Toep}(\tilde{\mathbf{a}})$, where

$$\tilde{a}_s := \frac{1}{n|R_s|} \sum_{l=1}^n \sum_{(j,k) \in R_s} x_j^{(l)} x_k^{(l)}. \quad (10)$$

Here, R_s is defined in Definition 1, and $|R_s|$ denotes its cardinality. In particular, if $R = [d]$, the estimator simplifies to

$$\tilde{T} = \text{avg} \left(\frac{1}{n} \sum_{l=1}^n \mathbf{x}^{(l)} \mathbf{x}^{(l)T} \right). \quad (11)$$

The non-asymptotic bounds of the estimator \tilde{T} have been extensively studied in [7, 21].

B. Dithered Quantization Scheme

Quantization refers to the process of mapping continuous inputs into a discrete form [30]. This technique is particularly useful for processing continuous data, as it enables the conversion of data into a discrete form with low resolution, thereby significantly reducing the costs associated with data processing and transmission [34, 35]. Consequently, quantization theory has received considerable attention, especially in the fields of statistical learning and estimation [36]. A key challenge in quantization lies in navigating the trade-off between achieving high approximation accuracy and minimizing the processing costs.

A common quantization scheme is the *dithered quantization scheme*, which introduces an appropriate random dither to the signal before quantization.

Definition 4: Let $\mathbf{x} \in \mathbb{R}^d$ denote the signal and $\boldsymbol{\tau} \in \mathbb{R}^d$ be a random dither (independent of \mathbf{x}) with i.i.d. entries sampled from some distribution. The dithered quantization is defined as

$$\dot{\mathbf{x}} = \mathcal{Q}_\Delta(\mathbf{x} + \boldsymbol{\tau}), \quad (12)$$

where

$$\mathcal{Q}_\Delta(x) := \Delta \left(\left\lfloor \frac{x}{\Delta} \right\rfloor + \frac{1}{2} \right) \in \Delta \cdot \left(\mathbb{Z} + \frac{1}{2} \right), \quad (13)$$

and $\mathcal{Q}_\Delta(\mathbf{x})$ denotes entry-wise quantization of \mathbf{x} .

Within this framework, several special designations are defined as follows.

- For a given quantization level $\Delta > 0$, the *uniform dither* $\boldsymbol{\tau} = [\tau_i]$ is defined as

$$\tau_i \sim \mathcal{U} \left(\left[-\frac{\Delta}{2}, \frac{\Delta}{2} \right] \right). \quad (14)$$

- For a given quantization level $\Delta > 0$, the *triangular dither* $\boldsymbol{\tau} = [\tau_i]$ is defined as

$$\tau_i \sim \mathcal{U} \left(\left[-\frac{\Delta}{2}, \frac{\Delta}{2} \right] \right) + \mathcal{U} \left(\left[-\frac{\Delta}{2}, \frac{\Delta}{2} \right] \right). \quad (15)$$

- The *quantization error* is defined as the difference between the input and output of the quantizer, i.e.,

$$\boldsymbol{\omega} := \dot{\mathbf{x}} - (\mathbf{x} + \boldsymbol{\tau}). \quad (16)$$

- The *quantization noise* is defined as the overall difference between original input \mathbf{x} and final output, i.e.,

$$\boldsymbol{\xi} := \dot{\mathbf{x}} - \mathbf{x} \quad (17)$$

In most cases, the distribution of quantization noise $\boldsymbol{\xi}$ is unknown, making it challenging to analyze the effects of quantization. Fortunately, this issue can be addressed by a fundamental result from [37], stated as follows.

Lemma 5: Let $\mathbf{x} = [x_i]$ be the input signal, and let $\boldsymbol{\tau} = [\tau_i]$ be the random dither, where the entries of $\boldsymbol{\tau}$ are i.i.d. copies of a random variable Y . We denote the complex unit by i . Then:

- Quantization Error:* Let $\boldsymbol{\omega} = \dot{\mathbf{x}} - (\mathbf{x} + \boldsymbol{\tau}) = [\omega_i]$ be the quantization error. If $f(u) := \mathbb{E}(\exp(iuY))$ satisfies $f\left(\frac{2\pi l}{\Delta}\right) = 0$ for all non-zero integers l , then:
 - x_i and ω_j are independent for all $i, j \in [N]$,
 - $\{\omega_j : j \in [N]\}$ are i.i.d. with distribution $\mathcal{U}\left(\left[-\frac{\Delta}{2}, \frac{\Delta}{2}\right]\right)$.
- Quantization Noise:* Let $\boldsymbol{\xi} = \dot{\mathbf{x}} - \mathbf{x} = [\xi_i]$ denote the quantization noise. Assume $Z \sim \mathcal{U}\left(\left[-\frac{\Delta}{2}, \frac{\Delta}{2}\right]\right)$ is independent of Y . Let $g(u) := \mathbb{E}(\exp(iuY))\mathbb{E}(\exp(iuZ))$. For a given positive integer p , if the p -th order derivative $g^{(p)}(u)$ satisfies

$$g^{(p)}\left(\frac{2\pi l}{\Delta}\right) = 0, \quad (18)$$

for all non-zero integers l . Then the p -th conditional moment of ξ_i does not depend on \mathbf{x} . Specifically,

$$\mathbb{E}[\xi_i^p | \mathbf{x}] = \mathbb{E}(Y + Z)^p. \quad (19)$$

It can be verified that both uniform dither and triangular dither satisfy the conditions of (a) in Lemma 5 [9, 37]. Moreover, triangular dither also satisfies the condition of (b) for $p = 2$. Under triangular dither, it is further known that

$$\mathbb{E}[\boldsymbol{\xi}\boldsymbol{\xi}^T] = \frac{\Delta^2}{4} \mathbf{I}_d, \quad (20)$$

which demonstrates that adding appropriate dither before quantization ensures that both the quantization error and quantization noise exhibit statistically desirable properties [8].

III. RULER-BASED QUANTIZED TOEPLITZ COVARIANCE ESTIMATION

In this section, we formally define the problem of quantized Toeplitz covariance estimation. Additionally, we propose an unbiased ruler-based estimator tailored for this setting, ensuring accurate estimation under the constraints of quantized data and sparse observation.

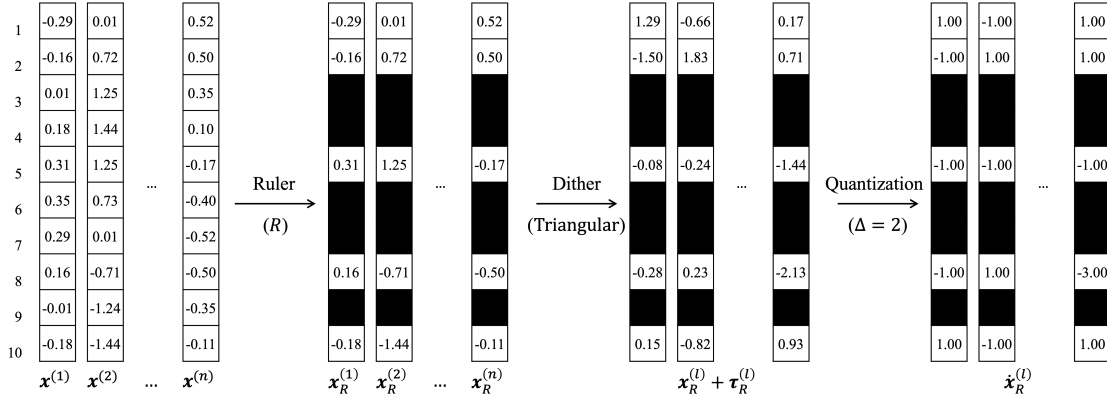


Fig. 2: Ruler-based quantized data in the RQTCE framework. In this example, we adopt the sparse ruler $R = \{1, 2, 5, 8, 10\}$ and employ triangular dither for quantization.

A. Problem Description

We aim to use the quantized data $\hat{x}^{(l)}$ for covariance estimation. Unlike previous studies on quantized covariance estimation, e.g., [8], our focus here is on the case where the covariance matrix is Toeplitz, and thus using the ruler-based method. Specifically, the problem can be formulated as follow.

Problem 6: Let $T \in \mathbb{R}^{d \times d}$ be a positive semidefinite symmetric Toeplitz matrix. $\mathbf{x}^{(1)}, \dots, \mathbf{x}^{(n)}$ are i.i.d. copies of a zero-mean, d -dimensional Gaussian random vector $\mathbf{x} \sim \mathcal{N}(0, T)$. For the quantization level $\Delta > 0$ and a ruler R , assume the availability of quantized data $\hat{\mathbf{x}}_R^{(l)}$, $l = 1, \dots, n$, where $\hat{\mathbf{x}}_R^{(l)}$ denotes the sub-vector of the quantized sample $\hat{\mathbf{x}}^{(l)}$ indexed by R . The goal of quantized Toeplitz covariance estimation is to return an estimator \hat{T} such that, with probability at least $1 - \delta$,

$$\|T - \hat{T}\|_2 \leq \epsilon \|T\|_2,$$

where $\|\cdot\|_2$ denotes the operator norm.

As illustrated in Fig. 2, the amount of information required for QTCE is minimal. Compared to the precise samples $\mathbf{x}^{(l)}$, we only rely on the quantized sub-vector $\hat{\mathbf{x}}_R^{(l)}$ to construct the estimator \hat{T} . Specifically, we neither have access to the precise information of the sample \mathbf{x}_R as in traditional Toeplitz covariance estimation [7], nor do we need to utilize all the information about $\hat{\mathbf{x}}$ as in other quantized covariance estimation methods [8]. This reduction in required information is due to the inherent properties of the Toeplitz covariance matrix.

B. Unbiased Estimator

To address Problem 6, we propose a slight modification to the ruler-based approach. Specifically, for the given quantization level $\Delta > 0$ and a given ruler R , inspired by (10), we define

$$\hat{a}_s^{(l)} = \frac{1}{|R_s|} \sum_{(j,k) \in R_s} \hat{x}_j^{(l)} \hat{x}_k^{(l)}, \quad (21)$$

for $s = 0, \dots, d-1$. It represents the quantized approximation for the covariance corresponding to the distance s .

In order to obtain an unbiased estimator, we first calculate the mean of $\hat{a}_s^{(l)}$. Recall that $\hat{x}_j^{(l)} = x_j^{(l)} + \xi_j^{(l)}$, we have

$$\begin{aligned} \mathbb{E}(\hat{a}_s^{(l)}) &= \frac{1}{|R_s|} \sum_{(j,k) \in R_s} \mathbb{E}(x_j^{(l)} x_k^{(l)}) \\ &= \frac{1}{|R_s|} \sum_{(j,k) \in R_s} \mathbb{E}((x_j^{(l)} + \xi_j^{(l)})(x_k^{(l)} + \xi_k^{(l)})). \end{aligned} \quad (22)$$

Note that T is a symmetric Toeplitz matrix, meaning that $T_{j,k}$ is constant for any $(j,k) \in R_s$. Thus we can write

$$\mathbb{E}(x_j^{(l)} x_k^{(l)}) = T_{j,k} \triangleq a_s, \quad (23)$$

where $s = |j - k|$. Further, under the *triangular dither* defined in (15), we know

$$\mathbb{E}(\xi_j^{(l)} \xi_k^{(l)}) = \frac{\Delta^2}{4} \delta_{j,k}, \quad (24)$$

where

$$\delta_{j,k} = \begin{cases} 1, & \text{if } j = k \\ 0, & \text{if } j \neq k \end{cases} \quad (25)$$

is the Dirac function. Meanwhile, by Lemma 5, we obtain

$$\begin{aligned} \mathbb{E}(x_j^{(l)} \xi_k^{(l)}) &= \mathbb{E}(x_j^{(l)} (\omega_k^{(l)} + \tau_k^{(l)})) \\ &= \mathbb{E}(x_j^{(l)} \omega_k^{(l)}) + \mathbb{E}(x_j^{(l)} \tau_k^{(l)}) = 0. \end{aligned} \quad (26)$$

It is known that $\mathbb{E}(x_k^{(l)} \xi_j^{(l)}) = \mathbb{E}(x_j^{(l)} \xi_k^{(l)}) = 0$ by symmetry. Thus combining all the above discussions, we conclude that

$$\begin{aligned} &\mathbb{E}((x_j^{(l)} + \xi_j^{(l)})(x_k^{(l)} + \xi_k^{(l)})) \\ &= \mathbb{E}(x_j^{(l)} x_k^{(l)}) + \mathbb{E}(x_j^{(l)} \xi_k^{(l)}) + \mathbb{E}(x_k^{(l)} \xi_j^{(l)}) + \mathbb{E}(\xi_j^{(l)} \xi_k^{(l)}) \\ &= a_s + \frac{\Delta^2}{4} \delta_s, \end{aligned} \quad (27)$$

which means $\mathbb{E}(\hat{a}_s^{(l)}) = a_s + \frac{\Delta^2}{4} \delta_s$. The result inspires us to define an estimator for T based on $\hat{a}_s^{(l)}$.

Definition 7: Under the settings in Problem 6, the bit efficient Toeplitz covariance estimator for T is defined as

$$\hat{T} = \text{Toep}(\hat{\mathbf{a}}) - \frac{\Delta^2}{4} I_d \triangleq \text{Toep}(\hat{\mathbf{a}}), \quad (28)$$

where

$$\hat{a}_s = \frac{1}{n} \sum_{l=1}^n \hat{a}_s^{(l)} = \frac{1}{n|R_s|} \sum_{l=1}^n \sum_{(j,k) \in R_s} \hat{x}_j^{(l)} \hat{x}_k^{(l)}, \quad (29)$$

is the average value of $\hat{a}_s^{(l)}$.

In the estimator \hat{T} , the term $\frac{\Delta^2}{4} I_d$ arises due to the introduction of the triangular dither. However, this does not mean that the triangular dither performs poorly. On the contrary, the use of triangular quantization enables us to calculate the second-order moments of the quantization noise $\xi^{(l)}$ and thus derive (27). Overall, when triangular dither is employed, \hat{T} serves as an appropriate estimator for T .

Theorem 8: Under the settings in Problem 6, if the triangular dither is employed, then

$$\mathbb{E}(\hat{T}) = T, \quad (30)$$

which means that the estimator \hat{T} defined in Definition 7 is unbiased.

Proof. Combining (27) with the fact

$$\hat{a}_s = \hat{a}_s - \frac{\Delta^2}{4} \delta_s = \frac{1}{n} \sum_{l=1}^n \hat{a}_s^{(l)} - \frac{\Delta^2}{4} \delta_s, \quad (31)$$

we can easily get (30). \blacksquare

Thus far, we have constructed an unbiased estimator of T . However, this construction alone does not fully resolve Problem 6. To provide a comprehensive solution, it is essential to further analyze the estimation error of \hat{T} . This crucial aspect will be the focus of the subsequent section.

IV. NON-ASYMPTOTIC PERFORMANCE ANALYSIS OF \hat{T}

In this subsection, we delve into the analysis of the non-asymptotic error bounds of \hat{T} . Building on this foundation, we further examine its rate of convergence. While this task presents significant challenges, it is essential for a comprehensive understanding of the estimator's performance.

A. Non-asymptotic Bounds of \hat{T}

We now proceed to analyze the error bounds of \hat{T} under both the maximum norm and the operator norm. For the maximum norm case, i.e., $\|T - \hat{T}\|_\infty = \max_{s \in [d]} |a_s - \hat{a}_s|$, which quantifies the entry-wise approximation accuracy of \hat{T} with respect to T . This metric is particularly useful for evaluating the performance of the estimator in approximating individual entries of the covariance matrix.

Theorem 9: Under the settings in Problem 6, for a given quantization level $\Delta > 0$, if a particular ruler R and the triangular dither is employed, there exists a universal constant $c > 0$ such that the estimator \hat{T} satisfies

$$\begin{aligned} & \mathbb{P}\{\|T - \hat{T}\|_\infty \geq t\} \\ & \leq 2|R| \exp \left[-cn \min \left(\frac{t^2}{K^2}, \frac{t}{K} \right) \right], \end{aligned} \quad (32)$$

where $K = 2(\|T\|_2 + 2\Delta^2)$. Especially, for any $\epsilon \in (0, 1]$, if we take $t = \epsilon \|T\|_\infty$, then

$$\mathbb{P}\{\|T - \hat{T}\|_\infty \geq \epsilon \|T\|_\infty\} \leq 2|R| \exp \left[-\frac{cn\epsilon^2 \|T\|_\infty^2}{K^2} \right]. \quad (33)$$

Proof. See Appendix A. \blacksquare

Theorem 9 demonstrates that our proposed estimator \hat{T} can approximate T with arbitrary accuracy in the entry-wise sense. This result provides partial evidence for the effectiveness of \hat{T} . Moreover, it plays a crucial role in analyzing the case when T is banded Toeplitz, as discussed in Section V.

Subsequently, we shift our focus to the error bounds in terms of the operator norm. Deriving non-asymptotic bounds for \hat{T} under this norm, however, is a challenging task. While it is known that $\hat{x} = x + \tau + \omega$, the intricate relationship between ω and τ leaves the distribution of \hat{x} uncertain. This uncertainty introduces significant challenges in directly leveraging existing theoretical frameworks. Therefore, an alternative approach is necessary to establish the desired bounds.

Fortunately, for Toeplitz matrices, the following fundamental result provides a useful tool for bounding their operator norm [38].

Lemma 10: Let $e = (e_0, \dots, e_{d-1})^T \in \mathbb{R}^d$. The operator norm of the Toeplitz matrix $\text{Toep}(e)$ can be bounded as

$$\|\text{Toep}(e)\|_2 \leq \sup_{x \in [0, 1]} L_e(x), \quad (34)$$

where the function $L_e(x)$ is defined as

$$L_e(x) = e_0 + 2 \sum_{s=1}^{d-1} e_s \cos(2\pi s x). \quad (35)$$

Lemma 10 provides a bound for the operator norm of a Toeplitz matrix by introducing the function $L_e(x)$. Consequently, it allows the operator norm for $T - \hat{T}$ to be transformed into the problem of analyzing the supremum of $L_e(x)$. Based on Lemma 10, we can derive the following theorem.

Theorem 11: For any $\epsilon \in (0, 1]$, assume that random vector $e \in \mathbb{R}^d$ satisfies the following conditions:

- 1) For any fixed $s \in [d]$,

$$\mathbb{P}\{|e_s| > 10t\} \leq 2e^{-f(t)}, \quad (36)$$

- 2) For any fixed $x \in [0, 1]$,

$$\mathbb{P}\left\{|L_e(x)| > \frac{\epsilon}{2}t\right\} \leq 2e^{-f(t)}, \quad (37)$$

where $t > 0$ and $f(t) > 0$. Then, there exists a universal constant $C > 0$ such that

$$\mathbb{P}\left\{\sup_{x \in [0, 1]} |L_e(x)| \leq \epsilon t\right\} > 1 - \frac{Cd^2}{\epsilon} e^{-f(t)}. \quad (38)$$

Proof. See Appendix B. \blacksquare

Theorem 11 provides a framework for deriving a non-asymptotic bound for \hat{T} . Specifically, it involves finding a suitable function $f(t)$ such that the generators e of the Toeplitz matrix $T - \hat{T}$ satisfy (36) and (37) when $t = \|T\|_2$. While this task is challenging, the underlying approach is inspired by the proof in [7]. By leveraging this method, we can successfully derive non-asymptotic bounds for \hat{T} .

Theorem 12: Under the settings in Problem 6, for a given quantization level $\Delta > 0$, if a particular ruler R and the triangular dither is employed, then for any $\epsilon \in (0, 1]$, let

$$\kappa = \frac{\epsilon^2 \|T\|_2^2}{(\|T\|_2^2 + \Delta^4) \phi(R)}, \quad (39)$$

and there exist universal constants $c, C > 0$ such that

$$\mathbb{P} \left\{ \|T - \hat{T}\|_2 > \epsilon \|T\|_2 \right\} \leq \frac{Cd^2}{\epsilon} \exp(-c n \kappa), \quad (40)$$

where \hat{T} is the estimator defined in Definition 7.

Proof. See Appendix C. \blacksquare

So far our results have been derived under the assumption that $\mathbf{x}^{(1)}, \dots, \mathbf{x}^{(n)}$ are Gaussian. We note that in the proofs, we mainly rely on their sub-Gaussian nature, meaning that the results can be readily generalized to the sub-Gaussian case with a minor adjustment to (79). This generalization ensures that our results offer a more general theoretical guarantee for \hat{T} . Furthermore, our proposed estimator \hat{T} demonstrates the capability to approximate T with arbitrary precision ϵ in terms of the operator norm. This result highlights the potential of performing covariance estimation using low-resolution data, making it particularly valuable in scenarios where data resolution is constrained by practical limitations.

B. Rate of Convergence

In the previous subsection, we established the error bound of the estimator \hat{T} through a detailed analysis. In this subsection, we proceed to analyze the rate of convergence of \hat{T} with respect to n . This theoretical result provides insights into the factors that influence the rate of convergence. Based on Theorem 12, we can straightforwardly obtain the following result.

Theorem 13: Under the conditions of Theorem 12, if we take

$$n = \Theta \left(\frac{\log(d/\epsilon\delta)}{\kappa} \right), \quad (41)$$

then $\|T - \hat{T}\|_2 \leq \epsilon \|T\|_2$ with probability at least $1 - \delta$.

From Theorem 13, it follows that the rate of convergence of \hat{T} is mainly determined by κ . A larger κ corresponds to a higher rate of convergence. Among κ in (39), the coverage coefficient $\phi(R)$ plays a significant role in influencing the rate of convergence. While it is challenging to analyze the value of $\phi(R)$ for a general ruler, for the ruler R_α defined in Definition 2, we have the following useful result in [7].

Lemma 14: For any $\alpha \in [1/2, 1]$, R_α satisfies $|R_\alpha| \leq 2d^\alpha$ and

$$\phi(R) \leq d^{2-2\alpha} + O(d^{1-\alpha} \cdot \log d). \quad (42)$$

Note that Lemma 14 is consistent with (9). Combining this lemma with Theorem 13, we have immediately the following theorem.

Theorem 15: Under the conditions of Theorem 12, if we use the ruler R_α and take

$$n = \mathcal{L} \cdot \Theta \left(\frac{\log(d/\epsilon\delta) \cdot \max\{d^{2-2\alpha}, d^{1-\alpha} \cdot \log d\}}{\epsilon^2} \right), \quad (43)$$

where $\mathcal{L} = \frac{\|T\|_2^2 + \Delta^4}{\|T\|_2^2}$. Then $\|T - \hat{T}\|_2 \leq \epsilon \|T\|_2$ with probability at least $1 - \delta$.

Notably, when $\Delta = 0$, we know $\mathcal{L} = 1$, and thus Theorem 15 reduces to [7, Theorem 4.4]. Remarkably, when $\Delta \neq 0$, the result in Theorem 15 is only slightly worse by a factor of \mathcal{L} . This result is significant, as it demonstrates that

even with the coarse data, we can achieve the same order of convergence as the unquantized case.

Remark 16: From Theorem 15, we observe the inherent trade-off between VSC, ESC, and resolution in Toeplitz covariance estimation. Specifically, VSC corresponds to the number of samples n , while ESC is related to the cardinality of the ruler R , which is closely tied to the coverage coefficient $\phi(R)$. The resolution, on the other hand, is determined directly by the quantization level Δ . A larger Δ implies a lower resolution. Theorem 15 demonstrates that reducing one or more of these quantities (VSC, ESC or resolution) necessitates compensatory increases in the remaining quantities to maintain the desired estimation accuracy. For instance, for a fixed ruler R , reducing the resolution of the data (i.e., increasing Δ) requires an increase in the number of samples (i.e., VSC) to achieve the same level of accuracy. This interplay highlights the necessity of balancing these factors in practical covariance estimation tasks.

To further illustrate the implications of Theorem 15, we examine two special cases: the *full ruler* R_1 and the *sparse ruler* $R_{1/2}$. These cases provide contrasting perspectives on the trade-offs between VSC, ESC and resolution. The results are summarized in the following corollary.

Corollary 17: Under the conditions of Theorem 12, it holds that $\|T - \hat{T}\|_2 \leq \epsilon \|T\|_2$ with probability at least $1 - \delta$ if any of the two conditions holds:

- 1) The full ruler R_1 is used with the VSC

$$n_1 = \mathcal{L} \cdot \Theta \left(\frac{\log d \cdot \log(d/\epsilon\delta)}{\epsilon^2} \right), \quad (44)$$

- 2) or, the sparse ruler $R_{1/2}$ is used with the VSC

$$n_{1/2} = \mathcal{L} \cdot \Theta \left(\frac{d \cdot \log(d/\epsilon\delta)}{\epsilon^2} \right), \quad (45)$$

where $\mathcal{L} = \frac{\|T\|_2^2 + \Delta^4}{\|T\|_2^2}$.

Corollary 17 demonstrates that for a preset accuracy ϵ and quantization level Δ , reducing the ESC from $|R_1| = d$ to $|R_{1/2}| = O(\sqrt{d})$ leads to a corresponding increase in VSC. Despite this trade-off, the results remain highly promising. When $R_{1/2}$ is employed, the proposed estimator \hat{T} achieves a

convergence rate of $O \left(\sqrt{\frac{d \log(d/\delta)}{n}} \right)$, which is comparable to the result in [8, Theorem 3] where the full ruler R_1 is used. Notably, quantization only affects the coefficients of the convergence rate, leaving the convergence order unchanged. These results strongly suggest that the proposed estimator \hat{T} is near optimal.

V. LOW-RANK AND BANDED CASES

For Toeplitz matrices, the low-rank and banded cases are of particular interest due to their prevalence in practical applications [3]. In this section, we focus on these two special cases by incorporating the low-rank and band-limit properties into the quantized Toeplitz covariance estimation problem. By leveraging these structural assumptions, we aim to achieve a faster rate of convergence compared to the general case.

A. Low-rank Case

Low-rankness is a property often considered in matrix analysis [39]. Therefore, we further explore the effect of low-rankness on the rate of convergence. However, upon examining the conclusion in Theorem 12, it appears that low-rankness cannot be directly related to the results presented there. So we have to make a slight modification to it.

For low-rank Toeplitz matrices, we rely on the following lemma from [7]:

Lemma 18: Let $\alpha \in [1/2, 1]$. Given positive semidefinite Toeplitz matrix $T \in \mathbb{R}^{d \times d}$ and the sparse ruler R_α defined in Definition 2, for any $k \leq d$ the following inequality holds

$$\|T_{R_\alpha}\|_2^2 \leq \frac{32k^2}{d^{2-2\alpha}} \cdot \|T\|_2^2 + 8\lambda(k, T), \quad (46)$$

where

$$\lambda(k, T) = \min(\|T - T_k\|_2^2, \frac{2}{d^{1-\alpha}} \cdot \|T - T_k\|_F^2). \quad (47)$$

Here, T_k is the best rank- k approximation of T satisfying

$$T_k = \arg \min_M \|T - M\|_F = \arg \min_M \|T - M\|_2, \quad (48)$$

where $\text{rank}(M) = k$.

Lemma 18 shows that for a rank- k Toeplitz matrix T , the operator norm of its principal submatrix T_{R_α} can be bounded by $\|T\|_2$, with the bound explicitly depending on k . Inspired by Lemma 18, a slight modification to the proof procedure of Theorem 12 leads to the following result.

Theorem 19: Under the conditions of Theorem 12, consider the low-rank case, where $\text{rank}(T) = k$. If we use the ruler R_α and take

$$n = \mathcal{L}' \cdot \Theta \left(\frac{\log(d/\epsilon\delta) \cdot \max\{d^{2-2\alpha}, d^{1-\alpha} \cdot \log d\}}{\epsilon^2} \right),$$

where $\mathcal{L}' = \frac{\lambda\|T\|_2^2 + \Delta^4}{\|T\|_2^2}$ and $\lambda = \frac{k^2}{d}$. Then $\|T - \hat{T}\|_2 \leq \epsilon\|T\|_2$ with probability at least $1 - \delta$.

Proof. See Appendix D. \blacksquare

It can be seen that Theorem 19 applies to the case where $k^2 < d$. This observation highlights that low-rankness can, in certain scenarios, significantly enhance the rate of convergence. We regard Theorem 19 as an illuminating result in this context.

Similarly, we can get the following corollary:

Corollary 20: Under the conditions of Theorem 12, consider the low-rank case, i.e., $\text{rank}(T) = k$. It holds that $\|T - \hat{T}\|_2 \leq \epsilon\|T\|_2$ with probability at least $1 - \delta$ if any of the two conditions holds:

- 1) The full ruler R_1 is used with the VSC

$$n_1 = \mathcal{L}' \cdot \Theta \left(\frac{\log d \cdot \log(d/\epsilon\delta)}{\epsilon^2} \right), \quad (49)$$

- 2) or, the sparse ruler $R_{1/2}$ is used with the VSC

$$n_{1/2} = \mathcal{L}' \cdot \Theta \left(\frac{d \cdot \log(d/\epsilon\delta)}{\epsilon^2} \right), \quad (50)$$

where $\mathcal{L}' = \frac{\lambda\|T\|_2^2 + \Delta^4}{\|T\|_2^2}$ and $\lambda = \frac{k^2}{d}$.

It is seen from Corollary 20 that low-rankness primarily influences the coefficient of convergence rate (i.e., \mathcal{L}'), rather than altering its scaling order. As $k < \sqrt{d}$, the presence of low-rankness accelerates the rate of convergence, offering substantial practical advantages. This result serves as an insightful and illuminating contribution to the study of quantized Toeplitz covariance estimation.

B. Banded Case

We now turn our attention to the banded case, a fundamental property that has been extensively studied in the context of Toeplitz covariance estimation [40]. In this setting, we assume that T is banded, meaning that only a limited number of diagonals near the main diagonal contain non-zero entries. Specifically, for the Toeplitz matrix $T = \text{Toep}(a)$, we define T to be banded if and only if there exists a positive integer $0 < m < d$ such that $a_s = 0$ for all $s \geq m$. A banded Toeplitz matrix naturally exhibits sparsity. Notably, a common approach to estimating sparse matrices is the thresholding procedure, as discussed in [3]. In this section, we leverage this technique to develop effective estimation methods tailored to the banded case.

Compared to the low-rank case, the banded case presents additional challenges. While the results for the low-rank case can be derived with a slight modification of the proof of Theorem 12, handling the banded case requires a more intricate approach. Specifically, we need to initiate a separate line of reasoning and consider the problem from a different perspective.

As mentioned before, the sparse case can be addressed using the thresholding method. Specifically, we consider the estimator $\check{T}_\zeta := \mathcal{T}_\zeta(T)$ for some threshold ζ , where

$$\mathcal{T}_\zeta(a) = a \cdot \mathbb{I}(|a| \geq \zeta),$$

and $\mathcal{T}_\zeta(\hat{T})$ denotes entry-wise thresholding applied to the matrix \hat{T} . Instead of \hat{T} , we will obtain the error bound on \check{T}_ζ .

We begin by addressing the estimation error of the zero diagonals. Specifically, for the Toeplitz matrix $T = \text{Toep}(a)$, the $(s+1)$ -th diagonal being zero implies that $a_s = 0$. With Theorem 9, we know that there exists a constant $C_1 > 0$ such that

$$|a_s - \hat{a}_s| < C_1 \mathcal{K} \quad (51)$$

with probability at least $1 - \delta$, where $\mathcal{K} = K \sqrt{\frac{\log(|R|/\delta)}{n}}$. Let $\zeta = C_2 \mathcal{K}$ with a sufficiently large $C_2 > C_1$ and define $\check{T}_\zeta = \text{Toep}(\check{a})$. We consider two cases:

- If $|\hat{a}_s| < \zeta$, then $\check{a}_s = 0$. In this case,

$$|a_s - \check{a}_s| = |a_s| \leq |a_s - \hat{a}_s| + |\hat{a}_s| \leq (C_1 + C_2) \mathcal{K}. \quad (52)$$
- If $|\hat{a}_s| \geq \zeta$, then $\check{a}_s = \hat{a}_s$. In this case,

$$|a_s - \check{a}_s| = |a_s - \hat{a}_s| \leq C_1 \mathcal{K}. \quad (53)$$

Additionally, note that

$$|a_s| \geq |\hat{a}_s| - |a_s - \hat{a}_s| \geq (C_2 - C_1) \mathcal{K}. \quad (54)$$

which implies that

$$|a_s - \check{a}_s| \leq \frac{C_1}{C_2 - C_1} |a_s|. \quad (55)$$

Combining the above results, we conclude

$$\mathbb{P} \{ |a_s - \check{a}_s| \leq C_3 \min(|a_s|, \mathcal{K}) \} \geq 1 - \delta, \quad (56)$$

where

$$C_3 \geq \max \left\{ 2C_2, \frac{C_1}{C_2 - C_1} \right\}. \quad (57)$$

This implies that if $a_s = 0$, then $\check{a}_s = 0$ with probability at least $1 - \delta$. This property provides valuable insights into the structure of the Toeplitz matrix and its estimation.

By leveraging this property, the estimation error under the operator norm can be effectively controlled (see Theorem 21). Specifically, for a banded Toeplitz matrix $T = \text{Toep}(\mathbf{a})$ with $a_s = 0$ for all $s \geq m$, this property significantly reduces the degrees of freedom in the estimation process. Such a structural simplification enables the threshold estimator \check{T}_ζ to achieve higher accuracy with fewer samples or lower resolution compared to the general case.

Utilizing this property, we derive a non-asymptotic bound on the estimation error $\|T - \check{T}_\zeta\|_2$ under the operator norm:

Theorem 21: Under the conditions of Theorem 12, we further assume that the bandwidth of T is m , i.e., $T = \text{Toep}(\mathbf{a})$ with $a_s = 0$ for all $s \geq m$. For $p > 1$, consider the ruler R and the thresholding estimator $\check{T}_\zeta = \mathcal{T}_\zeta(\hat{T})$ for

$$\zeta = CK \sqrt{\frac{\log |R| + 4p \log d}{n}} \quad (58)$$

with sufficiently large C . If $n = \Theta(\log |R| + 4p \log d)$, then with probability at least $1 - e^{-p}$ it holds that

$$\|T - \check{T}_\zeta\|_2 \leq C' K m \sqrt{\frac{\log |R| + 4p \log d}{n}}, \quad (59)$$

where $K = 2(\|T\|_2 + 2\Delta^2)$ and C' is a universal constant.

Proof. See Appendix E. ■

The derived constraints explicitly illustrate the dependence of the estimation error on the bandwidth m , the sample size n (i.e., VSC), the cardinality of the ruler R (i.e., ESC), and the quantization level Δ (i.e., relative to resolution). For a given error tolerance ϵ , the rate of convergence can achieve

$$K \cdot O \left(m \sqrt{\frac{\log |R| + 4p \log d}{n}} \right),$$

which is comparable to the results presented in [8, Theorem 4]. These findings demonstrate that incorporating the band-limit property not only enhances the rate of convergence but also reinforces the theoretical guarantees of the performance of \check{T}_ζ , aligning well with expectations.

Remark 22: Theorem 21 primarily applies to the scenario where T is known to be band-limited, but the exact bandwidth m is not specified. In the case that the bandwidth m is known, we can define the estimator as

$$\check{T} = \text{Toep}(\check{\mathbf{a}}), \quad (60)$$

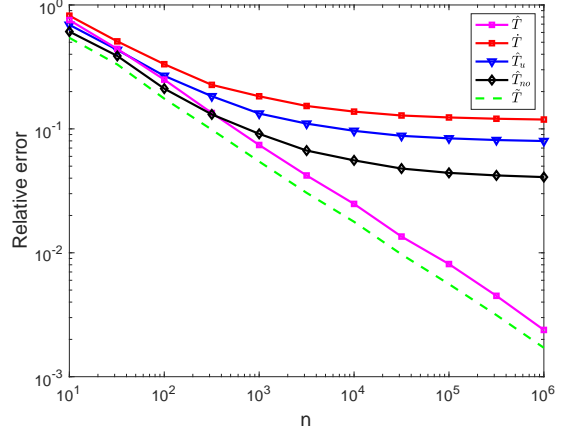


Fig. 3: Log-log curve of the relative error $\frac{\|\hat{T} - T\|}{\|T\|}$ with respect to the number of samples n

where the components of $\check{\mathbf{a}}$ are given by

$$\check{a}_s = \begin{cases} \hat{a}_s, & s < m \\ 0, & s \geq m \end{cases} \quad (61)$$

The estimator \check{T} defined in (60) also satisfies Theorem 21.

VI. NUMERICAL RESULTS

We validate our theoretical findings with numerical experiments in this section. Specifically, we use the Vandermonde decomposition to randomly generate Toeplitz matrices [41]. To be precise, generating a d -dimensional Toeplitz matrix involves the following steps for $k \leq d$:

- 1) Sampling k distinct frequencies from $\mathcal{U}([0, 1])$ and constructing a Fourier matrix $F_s \in \mathbb{C}^{d \times k}$;
- 2) Sample k independent values from $\mathcal{N}(0, 1)$, taking their absolute values as the amplitudes, and then forming a diagonal matrix D ;
- 3) Constructing the complex Toeplitz matrix as $T_c = F_s D F_s^*$.

We take $T = \text{real}(T_c)$ for numerical experiments. It should be noted that $\text{rank}(T) = \min\{d, 2k\}$ at this point.

In *Experiment 1*, a symmetric Toeplitz matrix $T \in \mathbb{R}^{16 \times 16}$ is randomly generated. The quantization level is set to $\Delta = 5$, and the ruler $R_{1/2} = \{1, 2, 3, 4, 8, 12, 16\}$ is employed to estimate T using several estimators:

- The proposed estimator \hat{T} : Triangular dither is applied, and $\frac{\Delta^2}{4} I_d$ is subtracted to mitigate the error introduced by the triangular dither.
- \check{T} : Triangular dither is applied without $\frac{\Delta^2}{4} I_d$ to mitigate the error introduced by the triangular dither.
- \hat{T}_u : Uniform dither is applied, and $\frac{\Delta^2}{6} I_d$ is subtracted to mitigate the error introduced by the uniform dither.
- \hat{T}_{no} : Quantization is applied without any dithering.
- \check{T} : No quantization is applied, serving as the benchmark.

We plot the log-log curve of the relative error versus the number of samples n in Fig. 3. The relative error of the proposed estimator decreases almost linearly with n in the

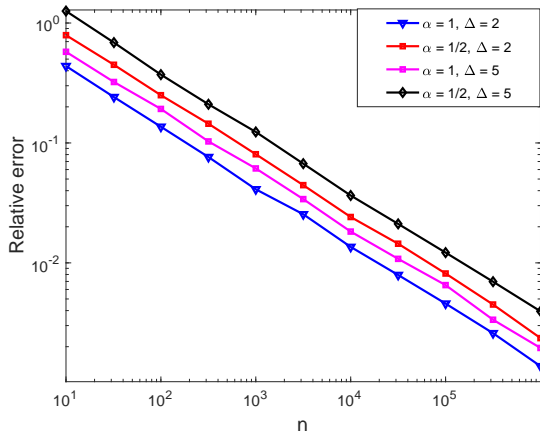


Fig. 4: Log-log curve of the relative error $\frac{\|\hat{T}-T\|}{\|T\|}$ changing with the number of samples n

log-log plot. In contrast, when uniform dither is used, or triangular dither is applied without correction, the relative error ceases to decrease significantly as the number of samples increases beyond a certain point. These results demonstrate that the proposed estimator \hat{T} can achieve arbitrary accuracy, even when relying solely on quantized coarse data. This highlights the superiority of \hat{T} in handling quantized data while maintaining high estimation accuracy.

In *Experiment 2*, we randomly generate 16-dimensional symmetric Toeplitz matrices and investigate the effect of the quantization level Δ and the choice of ruler on the estimation performance. Specifically, we consider two quantization levels, $\Delta = 2$ and $\Delta = 5$, using the sparse ruler $R_{1/2}$ and the full ruler R_1 , respectively. We examine the relationship between the relative error of \hat{T} and the number of samples n . The log-log curves of relative error versus n are plotted in Fig. 4 for all four cases. The results indicate that the curves are approximately straight lines with a slope of about -0.5007 , consistent with the theoretical convergence rate derived in Theorem 15. Additionally, these results illustrate the inherent trade-offs between VSC, ESC and resolution. For example, to achieve the same estimation accuracy, reducing the number of observed entries per sample (e.g., transitioning from the purple line to the black line) increases the error. This effect can be compensated for by increasing the resolution, as seen when transitioning from the black line to the red line. These observations confirm that achieving a preset estimation accuracy requires balancing VSC, ESC and resolution, and it is generally impossible to simultaneously reduce all three quantities.

In *Experiment 3*, we further investigate the impact of quantization level Δ on the estimation error for 16-dimensional symmetric Toeplitz matrices. Specifically, we fix the number of samples at $n = 1000$ and evaluate the performance of the estimator \hat{T} under three different rulers:

- The sparse ruler $R_{1/2} = \{1, 2, 3, 4, 8, 12, 16\}$.
- The sparse ruler

$$R_{3/4} = \{1, 2, 3, 4, 5, 6, 7, 8, 10, 12, 14, 16\}.$$

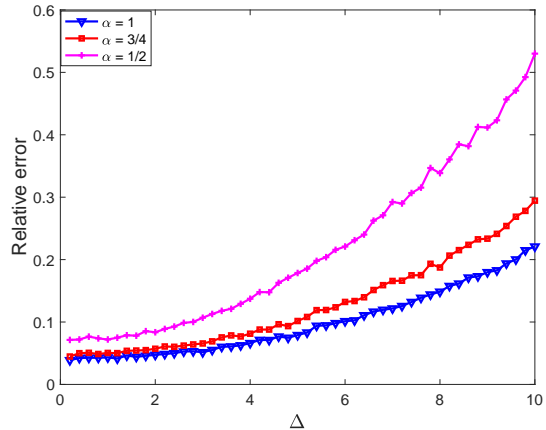


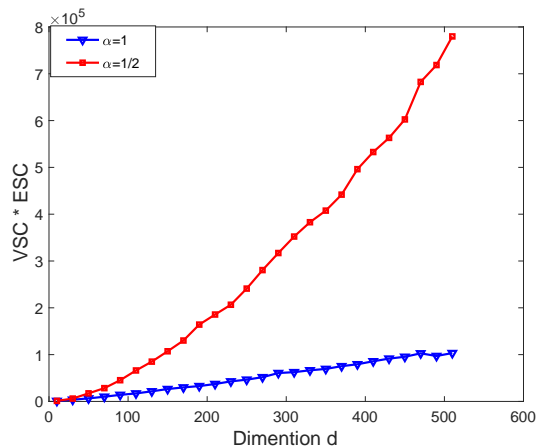
Fig. 5: The error variation curves corresponding to different quantization levels Δ

- The full ruler $R_1 = \{1, 2, \dots, 16\}$.

The error variation curves corresponding to different quantization levels Δ are plotted in Fig. 5. The results reveal that as Δ increases, the error initially varies more gently in the early stages and grows more noticeably in the later stages of the curve. This trend aligns closely with the theoretical description of \mathcal{L} in our analysis. These findings indicate that, within a certain range, increasing Δ , i.e., reducing data resolution, has a relatively limited impact on estimation accuracy. This demonstrates that the estimator maintains robustness against moderate reductions in data resolution, further supporting the feasibility of using quantized data for efficient covariance estimation.

In *Experiment 4*, we investigate the trade-off between VSC and ESC under a preset estimation accuracy of $\epsilon = 0.1$ and a fixed quantization level of $\Delta = 2$. Specifically, we evaluate the total sampling complexity, defined as the product of VSC and ESC, for two different rulers: the sparse ruler $R_{1/2}$ and the full ruler R_1 . The variation of total sampling complexity with the matrix dimension is plotted in Fig. 6. The results reveal contrasting trends between full-rank and low-rank matrices. For the full-rank case, while the sparse ruler $R_{1/2}$ effectively reduces the ESC, it leads to a significant increase in VSC, resulting in a sharp rise in total sampling complexity. In contrast, for low-rank matrices, where the rank is restricted to 10, the sparse ruler $R_{1/2}$ significantly outperforms the full ruler R_1 in terms of total sampling complexity when d is greater than 200. This highlights the advantage of using sparse rulers with low ESC in the covariance estimation of low-rank Toeplitz matrices. These findings provide valuable insights into optimizing the trade-offs between VSC and ESC under varying matrix properties.

In *Experiment 5*, we examine the behavior of \check{T}_ζ as defined in Theorem 21 within the context of a band-limited case. The sample size is set to $n = 1000$, and we assess the performance of the estimator \check{T}_ζ across various dimensions d . For the band-limited case, the bandwidth is fixed at $m = 5$. As shown in Fig. 7, the results indicate that the band-limited case achieves a smaller estimation error for the same number of samples.



(a) Full rank

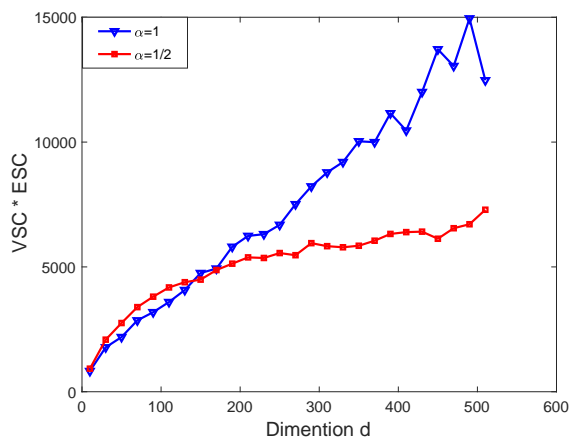
(b) rank(T) = 10

Fig. 6: Curve of total sample complexity with respect to data dimensionality required to achieve the preset accuracy $\epsilon = 0.1$

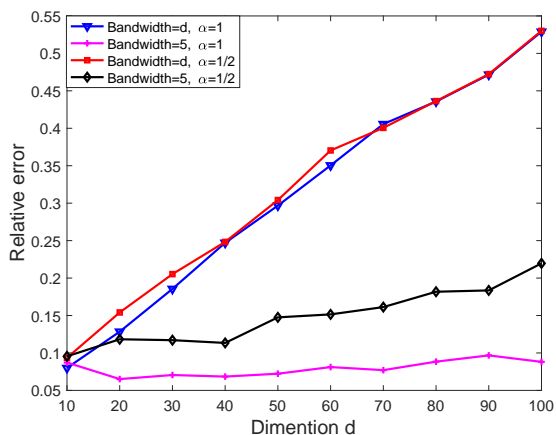


Fig. 7: Curve of the relative error versus dimension d for the band-limited case

Furthermore, once the bandwidth m is specified, the estimation error is essentially independent of d . These findings underscore the effectiveness of \hat{T}_ζ in estimating the band-limited Toeplitz

covariance matrix.

Overall, the results of our numerical experiments further validate the effectiveness of the proposed estimator \hat{T} . The experiments confirm that the convergence rate of \hat{T} with respect to the number of samples n is indeed $1/2$, aligning well with the theoretical predictions. Moreover, the results indicate that reducing the resolution of the data within a certain range has a relatively limited impact on the estimation error, demonstrating the robustness of the estimator under quantized data. Additionally, the trade-offs between VSC, ESC, and resolution are thoroughly examined through the numerical experiments. The findings highlight the intricate dependencies among these factors, illustrating how adjustments in one factor can be compensated by changes in others to achieve the desired estimation accuracy. These observations reinforce the practical value of our proposed estimator in balancing efficiency and accuracy in covariance estimation tasks.

VII. CONCLUSION

In this paper, we propose a ruler-based quantized Toeplitz covariance estimator capable of achieving highly accurate estimation of T by observing only a subset of each quantized coarse sample. We derive non-asymptotic error bounds for the estimator and further analyze the convergence rate of \hat{T} . Both theoretical analysis and experimental results confirm that the convergence order of the proposed estimator is $1/2$. Additionally, we demonstrate that reducing the resolution of the data within a certain range has a limited impact on the estimation accuracy. Our findings highlight the trade-offs between VSC, ESC and resolution, offering a balanced approach to covariance estimation with limited sample information. These results provide valuable insights and practical guidelines for achieving efficient and accurate covariance estimation in scenarios where data acquisition and processing resources are constrained.

Our exploration is based on Gaussian assumptions, which can be easily generalized to the sub-Gaussian case. However, extending this work to more general cases, such as heavy-tailed distributions, is a potential direction for future research. Additionally, in our analysis, the dither is required to follow a triangular distribution, which imposes a strong constraint. It is also interesting to investigate ways to relax this constraint, such as by restricting only certain features of the dither, in an effort to achieve similar effects through particular designs.

ACKNOWLEDGMENT

The authors would like to thank Prof. Michael Kwok-Po Ng of Hong Kong Baptist University for helpful comments that have improved the quality of the paper.

APPENDIX

A. Proof of Theorem 9

We first introduce Bernstein's inequality used to bound the sum of independent sub-exponential random variables [42].

$$|a_s - \hat{a}_s| = \left| a_s + \frac{\Delta^2}{4} \delta_s - \hat{a}_s \right| = \left| \frac{1}{n|R_s|} \sum_{l=1}^n \sum_{(j,k) \in R_s} \dot{x}_j^{(l)} \dot{x}_k^{(l)} - \frac{1}{|R_s|} \sum_{(j,k) \in R_s} \mathbb{E}(\dot{x}_j^{(l)} \dot{x}_k^{(l)}) \right|. \quad (63)$$

Lemma 23: Let X_1, \dots, X_n be independent sub-exponential random variables. Then, for every $t > 0$, we have

$$\begin{aligned} \mathbb{P}\left\{ \left| \frac{1}{n} \sum_{l=1}^n X_l - \mathbb{E}(X_i) \right| \geq t \right\} \\ \leq 2 \exp \left[-cn \min \left(\frac{t^2}{K^2}, \frac{t}{K} \right) \right], \end{aligned} \quad (62)$$

where $K = \max_l \|X_l\|_{\psi_1}$.

Now, we turn to the proof of Theorem 9. For any $s = 0, \dots, d-1$, we first consider the bound for $|a_s - \hat{a}_s|$, i.e., the bound for (63).

To bound (63), consider the case for any $(j, k) \in R_s$. We first bound

$$\left| \frac{1}{n} \sum_{l=1}^n \dot{x}_j^{(l)} \dot{x}_k^{(l)} - \mathbb{E}(\dot{x}_j^{(l)} \dot{x}_k^{(l)}) \right|.$$

Note that

$$\begin{aligned} \|\dot{x}_j^{(l)}\|_{\psi_2} &= \|x_j^{(l)} + \omega_j^{(l)} + \tau_j^{(l)}\|_{\psi_2} \\ &\leq \|x_j^{(l)}\|_{\psi_2} + \|\omega_j^{(l)}\|_{\psi_2} + \|\tau_j^{(l)}\|_{\psi_2} \\ &\leq \sqrt{T_{j,j}} + 2\Delta \\ &\leq \|T\|_2^{1/2} + 2\Delta, \end{aligned} \quad (64)$$

which means $\dot{x}_j^{(l)}$ and $\dot{x}_k^{(l)}$ are sub-Gaussian random variables. Hence, $\dot{x}_j^{(l)} \dot{x}_k^{(l)}$ is a sub-exponential random variable satisfying

$$\begin{aligned} \|\dot{x}_j^{(l)} \dot{x}_k^{(l)}\|_{\psi_1} &\leq \|\dot{x}_j^{(l)}\|_{\psi_2} \|\dot{x}_k^{(l)}\|_{\psi_2} \\ &\leq (\|T\|_2^{1/2} + 2\Delta)^2 \leq 2(\|T\|_2 + 2\Delta^2). \end{aligned} \quad (65)$$

By Bernstein's inequality, there exists a universal constant $c > 0$ such that

$$\begin{aligned} \mathbb{P}\left\{ \left| \frac{1}{n} \sum_{l=1}^n \dot{x}_j^{(l)} \dot{x}_k^{(l)} - \mathbb{E}(\dot{x}_j^{(l)} \dot{x}_k^{(l)}) \right| \geq t \right\} \\ \leq 2 \exp \left[-cn \min \left(\frac{t^2}{K^2}, \frac{t}{K} \right) \right] \end{aligned} \quad (66)$$

holds, where $K = 2(\|T\|_2 + 2\Delta^2)$. Substituting this result back into (63), we have

$$\mathbb{P}\{|a_s - \hat{a}_s| \geq t\} \leq 2|R_s| \exp \left[-cn \min \left(\frac{t^2}{K^2}, \frac{t}{K} \right) \right]. \quad (67)$$

Combining (67) with the fact $|R_s| \leq |R|$, we conclude the proof of Theorem 9.

B. Proof of Theorem 11

By (36), we can get a union bound over $s \in [d]$,

$$\mathbb{P}\{\exists s \in [d] : |e_s| > 10t\} \leq 2de^{-f(t)}. \quad (68)$$

And similarly, if we take $N = \{0, \frac{1}{Qd^2}, \frac{2}{Qd^2}, \dots, 1\}$ for $Q = 80\pi$, then

$$\mathbb{P}\left\{ \exists x \in N : |L_e(x)| > \frac{\epsilon}{2} t \right\} \leq \frac{3Qd^2}{\epsilon} e^{-f(t)}. \quad (69)$$

Thus the event

$$\mathcal{A} : |e_s| \leq 10t, \forall e \in [d], \text{ and } |L_e(x)| \leq \frac{\epsilon}{2} t, \forall x \in N \quad (70)$$

occurs with probability at least

$$1 - \frac{4Qd^2}{\epsilon} \cdot e^{-f(t)}.$$

For any $x \in [0, 1]$, we can find an $x' \in N$ such that $0 \leq x - x' < \frac{\epsilon}{Qd^2}$. And then condition on the event \mathcal{A} , we know

$$\begin{aligned} |L_e(x)| &\leq |L_e(x')| + |x - x'| \sup_{y \in [x', x]} |L'(y)| \\ &< \frac{\epsilon}{2} t + 40\pi d^2 t \cdot \frac{\epsilon}{Qd^2} = \epsilon t, \end{aligned} \quad (71)$$

where the second inequality holds because

$$\begin{aligned} |L'_e(y)| &= \left| 4\pi \sum_{s=1}^{d-1} s e_s \sin(2\pi s y) \right| \\ &\leq 4\pi d^2 \|e\|_\infty \leq 40\pi d^2 t. \end{aligned} \quad (72)$$

It is to say,

$$\mathbb{P}\{\exists x \in [0, 1] : |L_e(x)| > \epsilon t\} \leq \frac{Cd^2}{\epsilon} e^{-f(t)}, \quad (73)$$

where $C = 4Q$. This equation can be expressed equivalently as (38).

C. Proof of Theorem 12

We first introduce Hanson-Wright inequality [42]. This inequality is used to control the tail behavior of quadratic forms of sub-Gaussian random variables.

Lemma 24: Let $\mathbf{X} = (X_1, \dots, X_d)$ be a random vector with independent, zero-mean, sub-Gaussian coordinates. Let A be an $d \times d$ matrix. Then, for every $t \geq 0$, we have

$$\begin{aligned} \mathbb{P}\left\{ |\mathbf{X}^T A \mathbf{X} - \mathbb{E}(\mathbf{X}^T A \mathbf{X})| > t \right\} \\ \leq 2 \exp \left[-c \min \left(\frac{t^2}{K^4 \|A\|_F^2}, \frac{t}{K^2 \|A\|} \right) \right], \end{aligned} \quad (74)$$

where $K = \max_i \|X_i\|_{\psi_2}$.

Then, we turn to the prove Theorem 12. Observe that $T - \hat{T} = T - \text{Toep}(\hat{\mathbf{a}})$ is also a symmetric Toeplitz matrix. Let \mathbf{e} denote its associated generating vector. Since the distribution of \mathbf{x} is unknown, the proof involves non-trivial steps, which we complete as follows.

On the one hand, for any $s = 0, \dots, d-1$, we know

$$\begin{aligned} e_s &= a_s - \hat{a}_s \\ &= \frac{1}{n|R_s|} \sum_{l=1}^n \sum_{(j,k) \in R_s} \left(T_{j,k} + \frac{\Delta^2}{4} \delta_s - \dot{x}_j^{(l)} \dot{x}_k^{(l)} \right). \end{aligned} \quad (75)$$

We first calculate

$$\mathbb{E}[(\dot{x}_j^{(l)} \dot{x}_k^{(l)})^2] \leq \frac{1}{2} \left(\mathbb{E}[(\dot{x}_j^{(l)})^4] + \mathbb{E}[(\dot{x}_k^{(l)})^4] \right), \quad (76)$$

where

$$\begin{aligned} \mathbb{E}[(\dot{x}_j^{(l)})^4] &= \mathbb{E}[(x_j^{(l)} + \xi_j^{(l)})^4] \\ &\leq 8 \left(\mathbb{E}[(x_j^{(l)})^4] + \mathbb{E}[(\xi_j^{(l)})^4] \right). \end{aligned} \quad (77)$$

And we also have

$$\begin{aligned} |\xi_j^{(l)}| &= |\omega_j^{(l)} + \tau_j^{(l)}| \\ &\leq |\omega_j^{(l)}| + |\tau_j^{(l)}| \\ &\leq \frac{\Delta}{2} + \Delta \\ &= \frac{3\Delta}{2}. \end{aligned} \quad (78)$$

Moreover, by Isserlis's theorem, we know

$$\mathbb{E}[(x_j^{(l)})^4] \leq 3T_{j,j}^2 \leq 3\|T\|_2^2. \quad (79)$$

Combining the above, we derive that

$$\mathbb{E}[(\dot{x}_j^{(l)} \dot{x}_k^{(l)})^2] \leq 24\|T\|_2^2 + \frac{81}{2}\Delta^4. \quad (80)$$

Meanwhile, we know $\dot{x}_j^{(l)}$ is sub-Gaussian (by (64)). Considering the sub-Gaussian nature of $\dot{x}_j^{(l)}$, we confirm that $\dot{x}_j^{(l)} \dot{x}_k^{(l)}$ is sub-exponential. Combining with $\mathbb{E}(e_s) = 0$ and

$$\mathbb{E}(e_s^2) \leq \frac{1}{n} \left(24\|T\|_2^2 + \frac{81}{2}\Delta^4 \right), \quad (81)$$

we apply the sub-exponential tail bound

$$\mathbb{P}(|e_s| > 10\|T\|_2) \leq 2 \exp\left(-\frac{10\|T\|_2^2}{2\nu^2}\right), \quad (82)$$

where

$$\nu^2 = \frac{1}{n} \left(24\|T\|_2^2 + \frac{81}{2}\Delta^4 \right). \quad (83)$$

Thus,

$$\mathbb{P}\{|e_s| > 10\|T\|_2\} \leq 2 \exp(-cn\kappa). \quad (84)$$

On the other hand, for a fixed $x \in [0, 1]$, we associate it to a Toeplitz matrix $M \in \mathbb{R}^{d \times d}$, where

$$M_{j,k} = \frac{\cos(2\pi sx)}{|R_s|}, \quad s = |j-k| \in [d]. \quad (85)$$

Then,

$$\begin{aligned} L_e(x) &= e_0 + 2 \sum_{s=0}^{d-1} e_s \cos(2\pi sx) \\ &= \text{tr}(T_R - \hat{T}_R, M_R). \end{aligned} \quad (86)$$

Furthermore, let

$$\bar{T} = \frac{1}{n} \sum_{l=1}^n \dot{x}^{(l)} \dot{x}^{(l)T} - \frac{\Delta^2}{4} I_d, \quad (87)$$

we can see that $\hat{T} = \text{avg}(\bar{T})$. Thus,

$$\sum_{(j,k) \in R \times R: |j-k|=s} \hat{T}_{j,k} = \sum_{(j,k) \in R \times R: |j-k|=s} \bar{T}_{j,k}, \quad (88)$$

and then,

$$\begin{aligned} \text{tr}(\hat{T}_R, M_R) &= \sum_{(j,k) \in R \times R} \hat{T}_{j,k} M_{j,k} \\ &= \sum_{s=0}^{d-1} \sum_{(j,k) \in R \times R: |j-k|=s} \hat{T}_{j,k} M_{j,k} \\ &= \sum_{s=0}^{d-1} \sum_{(j,k) \in R \times R: |j-k|=s} \bar{T}_{j,k} M_{j,k} \\ &= \text{tr}(\bar{T}_R, M_R). \end{aligned} \quad (89)$$

Let $\dot{\Sigma} = \mathbb{E}(\dot{x}^{(l)T} \dot{x}^{(l)}) = T + \frac{\Delta^2}{4} I_d$, we can get

$$\begin{aligned} L_e(x) &= \text{tr}(T_R - \hat{T}_R, M_R) \\ &= \text{tr}(\dot{\Sigma}_R, M_R) - \frac{1}{n} \sum_{l=1}^n \dot{x}_R^{(l)T} M_R \dot{x}_R^{(l)}. \end{aligned} \quad (90)$$

We can also calculate that

$$\mathbb{E}(\dot{x}_R^{(l)T} M_R \dot{x}_R^{(l)}) = \text{tr}(\dot{\Sigma}_R, M_R). \quad (91)$$

Combining (91) with Hanson-Wright inequality, we get (92), where the last inequality holds because $\|M_R\|_2 \leq \phi R$.

Let $t = \frac{\epsilon}{2}\|T\|_2$ in (92). We can immediately get

$$\mathbb{P}\left\{|L_e(x)| > \frac{\epsilon}{2}\|T\|_2\right\} \leq 2 \exp(-cn\kappa). \quad (93)$$

Combining (84) and (93) with Theorem 11, we know there exists a universal constant $C > 0$ such that

$$\mathbb{P}\left\{\sup_{x \in [0,1]} |L_e(x)| \leq \epsilon\|T\|_2\right\} > 1 - \frac{Cd^2}{\epsilon} \exp(-cn\kappa). \quad (94)$$

With the help of Lemma 10, we can further know

$$\mathbb{P}\left\{\|T - \hat{T}\|_2 > \epsilon\|T\|_2\right\} \leq \frac{Cd^2}{\epsilon} \exp(-cn\kappa), \quad (95)$$

completing the proof.

D. Proof of Theorem 19

For a given ruler R_α , if $j, k \in R_\alpha$, then $T_{j,k} \leq \|T_{R_\alpha}\|_2$. Furthermore, (64) can be optimized as

$$\|\dot{x}_j^{(l)}\|_{\psi_2} \leq \|T_{R_\alpha}\|_2^{1/2} + 2\Delta, \quad (96)$$

and (80) can be optimized as

$$\mathbb{E}[(\dot{x}_j^{(l)} \dot{x}_k^{(l)})^2] \leq 24\|T_{R_\alpha}\|_2^2 + \frac{81}{2}\Delta^4. \quad (97)$$

Using derivations similar to those in the proof of Theorem 12 (see Appendix C), we have

$$\mathbb{P}\{|e_s| > 10\|T\|_2\} \leq 2 \exp(-cn\kappa) \quad (98)$$

and

$$\mathbb{P}\left\{|L_e(x)| > \frac{\epsilon}{2}\|T\|_2\right\} \leq 2 \exp(-cn\kappa'), \quad (99)$$

$$\begin{aligned}
\mathbb{P}\{|L_e(x)| > t\} &= \mathbb{P}\left\{\left|\mathrm{tr}(\dot{\Sigma}, M_R) - \frac{1}{n} \sum_{l=1}^n \dot{\mathbf{x}}_R^{(l)T} M_R \dot{\mathbf{x}}_R^{(l)}\right| > t\right\} \\
&\leq 2 \exp\left[-cn \min\left(\frac{t^2}{(\|T\|_2^{1/2} + 2\Delta)^4 \|M_R\|_F^2}, \frac{t}{(\|T\|_2^{1/2} + 2\Delta)^2 \|M_R\|}\right)\right] \\
&\leq 2 \exp\left[-cn \min\left(\frac{t^2}{(\|T\|_2^{1/2} + 2\Delta)^4 \phi(R)}, 1\right)\right]
\end{aligned} \tag{92}$$

$$\begin{aligned}
\left(\sum_{s=0}^{d-1} |a_s - \check{a}_s| \mathbb{I}(\mathcal{B}_s^C)\right)^p &\leq \left(\sum_{s=0}^{d-1} |a_s - \hat{a}_s| \mathbb{I}(\mathcal{B}_s^C) + \sum_{s=0}^{d-1} |\hat{a}_s - \check{a}_s| \mathbb{I}(|\hat{a}_s| < \zeta) \mathbb{I}(\mathcal{B}_s^C)\right)^p \\
&\leq (2d)^p \left(\sum_{s=0}^{d-1} |a_s - \hat{a}_s|^p \mathbb{I}(\mathcal{B}_s^C) + \sum_{s=0}^{d-1} |\hat{a}_s|^p \mathbb{I}(|\hat{a}_s| < \zeta) \mathbb{I}(\mathcal{B}_s^C)\right).
\end{aligned} \tag{105}$$

where $\kappa' = \min\left(\frac{\epsilon^2 \|T\|_2^2}{(\|T_{R_\alpha}\|_2^2 + \Delta^4) \phi(R_\alpha)}, 1\right)$. And combining with Theorem 11, we have

$$\mathbb{P}\left\{\sup_{x \in [0,1]} |L_e(x)| \leq \epsilon \|T\|_2\right\} > 1 - \frac{Cd^2}{\epsilon} \exp(-cn\kappa'). \tag{100}$$

and then,

$$\mathbb{P}\{\|T - \hat{T}\|_2 > \epsilon \|T\|_2\} \leq \frac{Cd^2}{\epsilon} \exp(-cn\kappa'). \tag{101}$$

Theorem 19 can be immediately get with the help of Lemma 18.

E. Proof of Theorem 21

Our goal is to bound $\mathbb{E}\|T - \check{T}_\zeta\|^p$. Define the event

$$\mathcal{B}_s : |a_s - \check{a}_s| \leq C_3 \min(|a_s|, \mathcal{K}), \tag{102}$$

and note that

$$\begin{aligned}
&\mathbb{E}\|T - \check{T}_\zeta\|^p \\
&\leq \mathbb{E}\left(\sum_{s=0}^{d-1} |a_s - \check{a}_s| \mathbb{I}(\mathcal{B}_s) + \sum_{s=0}^{d-1} |a_s - \check{a}_s| \mathbb{I}(\mathcal{B}_s^C)\right)^p \\
&\leq 2^p \mathbb{E}\left(\sum_{s=0}^{d-1} |a_s - \check{a}_s| \mathbb{I}(\mathcal{B}_s)\right)^p \\
&\quad + 2^p \mathbb{E}\left(\sum_{s=0}^{d-1} |a_s - \check{a}_s| \mathbb{I}(\mathcal{B}_s^C)\right)^p.
\end{aligned} \tag{103}$$

(a) When \mathcal{B}_s holds, i.e., $\mathbb{I}(\mathcal{B}_s) = 1$, we know that if $a_s = 0$, then $\check{a}_s = 0$. By the banded assumption on \mathbf{a} , it follows that

$$\mathbb{E}\left(\sum_{s=0}^{d-1} |a_s - \check{a}_s| \mathbb{I}(\mathcal{B}_s)\right)^p \leq (C_3 m \mathcal{K})^p. \tag{104}$$

(b) Considering the case where \mathcal{B}_s does not hold, i.e., $\mathbb{I}(\mathcal{B}_s^C) = 1$. In this case, we observe that (105) holds. Therefore, we have (106). We bound the two terms on the right-hand side of (106) separately.

We deal with the first term of (106) first. By Cauchy-Schwarz inequality, we know

$$\mathbb{E}[|a_s - \hat{a}_s|^p \mathbb{I}(\mathcal{B}_s^C)] \leq \sqrt{\mathbb{E}[|a_s - \hat{a}_s|^{2p}] \cdot \mathbb{P}(\mathcal{B}_s^C)}. \tag{107}$$

By Theorem 9, we know

$$\mathbb{P}\{|a_s - \hat{a}_s| \geq t\} \leq 2|R| \exp\left[-cn \min\left(\frac{t^2}{K^2}, \frac{t}{K}\right)\right], \tag{108}$$

which implies (109). where the last equation is because $\Gamma(p+1) \leq p^p$. Combining (109) with the fact $\mathbb{P}(\mathcal{B}_s^C) \leq \delta$, we further know

$$\begin{aligned}
&\mathbb{E}[|a_s - \hat{a}_s|^p \mathbb{I}(\mathcal{B}_s^C)] \\
&\leq \sqrt{\left(\frac{2|R|K^{2p}}{(cn)^p} \cdot p^p + \frac{2|R|K^{2p}}{(cn)^{2p}} \cdot (2p)^{2p}\right) \cdot \delta} \\
&= \sqrt{2|R|\delta} \cdot K^p \cdot \sqrt{\frac{p^p}{(cn)^p} + \frac{(2p)^{2p}}{(cn)^{2p}}}.
\end{aligned} \tag{110}$$

If we assume $\delta < \frac{1}{d^4}$ and take $p = -\frac{\log(\delta)}{4 \log d} > 1$, we further know

$$\begin{aligned}
&\mathbb{E}[|a_s - \hat{a}_s|^p \mathbb{I}(\mathcal{B}_s^C)] \\
&\leq 2\sqrt{|R|\delta} \left(K \sqrt{\frac{\log(1/\delta)}{cn}}\right) \\
&\leq 2d^{-p} (C_4 \mathcal{K})^p
\end{aligned} \tag{111}$$

with $C_4 = 1/\sqrt{c}$, where the last inequality holds because $|R| < d$ and $p > 1$.

We now turn to the second term of (106). $|\hat{a}_s| < \zeta$ means $|\check{a}_s| = 0$ and thus \mathcal{B}_s^C implies

$$\begin{aligned}
|a_s| &= |a_s - \check{a}_s| > C_3 \mathcal{K} > 2\zeta \\
&> 2|\hat{a}_s| \geq 2|a_s| - 2|a_s - \hat{a}_s|,
\end{aligned} \tag{112}$$

where the second inequality holds because $C_3 > 2C_2$ in (57). Thus

$$\frac{1}{2}|a_s| < |a_s - \check{a}_s|, \tag{113}$$

$$\mathbb{E} \left(\sum_{s=0}^{d-1} |a_s - \check{a}_s| \mathbb{I}(\mathcal{B}_s^C) \right)^p \leq (2d)^p \left(\sum_{s=0}^{d-1} \mathbb{E} [|a_s - \hat{a}_s|^p \mathbb{I}(\mathcal{B}_s^C)] + \sum_{s=0}^{d-1} \mathbb{E} [|\hat{a}_s|^p \mathbb{I}(|\hat{a}_s| < \zeta) \mathbb{I}(\mathcal{B}_s^C)] \right). \quad (106)$$

$$\begin{aligned} \mathbb{E} [|a_s - \hat{a}_s|^{2p}] &= 2p \int_0^\infty t^{2p-1} \mathbb{P} \{ |a_s - \hat{a}_s| \geq t \} dt \\ &\leq 4p|R| \int_0^\infty t^{2p-1} \exp \left[-cn \min \left(\frac{t^2}{K^2}, \frac{t}{K} \right) \right] dt \\ &= 4p|R| \int_0^K t^{2p-1} \exp \left(-cn \frac{t^2}{K^2} \right) dt + 4p|R| \int_K^\infty t^{2p-1} \exp \left(-cn \frac{t}{K} \right) dt \\ &\leq 4p|R| \int_0^\infty t^{2p-1} \exp \left(-cn \frac{t^2}{K^2} \right) dt + 4p|R| \int_0^\infty t^{2p-1} \exp \left(-cn \frac{t}{K} \right) dt \\ &\leq \frac{2p|R|K^{2p}}{(cn)^p} \cdot \Gamma(p) + \frac{4p|R|K^{2p}}{(cn)^{2p}} \cdot \Gamma(2p) \\ &\leq \frac{2|R|K^{2p}}{(cn)^p} \cdot p^p + \frac{2|R|K^{2p}}{(cn)^{2p}} \cdot (2p)^{2p}, \end{aligned} \quad (109)$$

which is to say,

$$\begin{aligned} &\mathbb{E} [|\hat{a}_s|^p \mathbb{I}(|\hat{a}_s| < \zeta) \mathbb{I}(\mathcal{B}_s^C)] \\ &\leq \zeta^p \mathbb{P} \left\{ |a_s - \hat{a}_s| > \frac{1}{2} |a_s| \right\}. \end{aligned} \quad (114)$$

And we also know $|a_s| > 2\zeta$. With the help of Theorem 9, we get

$$\begin{aligned} &\mathbb{P} \left\{ |a_s - \hat{a}_s| > \frac{1}{2} |a_s| \right\} \\ &\leq 2|R| \exp \left[-cn \min \left(\frac{|a_s|^2}{4K^2}, \frac{|a_s|}{2K} \right) \right] \\ &= 2|R| \exp \left[-cn \frac{\zeta^2}{K^2} \right] \\ &\leq 2|R| \exp \left[-cC_2^2 \log(|R|/\delta) \right] \\ &= 2|R| \cdot (\delta/|R|) \\ &= 2\delta. \end{aligned} \quad (115)$$

Thus

$$\mathbb{E} [|\hat{a}_s|^p \mathbb{I}(|\hat{a}_s| < \zeta) \mathbb{I}(\mathcal{B}_s^C)] \leq 2\delta \zeta^p \leq 2d^{-4p} (C_3 \mathcal{K})^p. \quad (116)$$

Combining all the above discussions, we know

$$\begin{aligned} &\mathbb{E} \|T - \check{T}_\zeta\|_2^p \\ &\leq (2C_3 m \mathcal{K})^p + 2 \cdot (4C_4 \mathcal{K})^p + 2 \cdot (4C_3 d^{-3} \mathcal{K}) \\ &\leq (C_5 m \mathcal{K})^p, \end{aligned} \quad (117)$$

where $C > 0$. Furthermore, by Markov's inequality,

$$\mathbb{P}(\|T - \check{T}_\zeta\|_2 \geq C_5 es \mathcal{K}) \leq \frac{\mathbb{E} \|T - \check{T}_\zeta\|_2^p}{(C_5 es \mathcal{K})^p} = e^{-p}. \quad (118)$$

Theorem 21 can be obtained by taking $\delta = d^{-4p}$.

REFERENCES

- [1] H. Krim and M. Viberg, "Two decades of array signal processing research: the parametric approach," *IEEE Signal Process. Mag.*, vol. 13, no. 4, pp. 67–94, Jul. 1996.
- [2] J. Dahmen, D. Keyzers, M. Pitz, and H. Ney, "Structured covariance matrices for statistical image object recognition," in *Mustererkennung*. Springer, Sep. 2000, pp. 99–106.
- [3] J. Maly, T. Yang, S. Dirksen, H. Rauhut, and G. Caire, "New challenges in covariance estimation: multiple structures and coarse quantization," in *Compressed Sensing in Inf. Process.* Springer, 2022, pp. 77–104.
- [4] Y. Ke, S. Minsker, Z. Ren, Q. Sun, and W.-X. Zhou, "User-friendly covariance estimation for heavy-tailed distributions," *Statist. Sci.*, vol. 34, no. 3, pp. 454–471, Mar. 2019.
- [5] Z. Yang, J. Li, P. Stoica, and L. Xie, "Sparse methods for direction-of-arrival estimation," in *Academic Press Library in Signal Processing, Cambridge, MA, USA: Academic Press*. Elsevier, 2018, pp. 509–581.
- [6] M. J. Brookes, J. Vrba, S. E. Robinson, C. M. Stevenson, A. M. Peters, G. R. Barnes, A. Hillebrand, and P. G. Morris, "Optimising experimental design for MEG beamformer imaging," *Neuroimage*, vol. 39, no. 4, pp. 1788–1802, 2008.
- [7] Y. C. Eldar, J. Li, C. Musco, and C. Musco, "Sample efficient toeplitz covariance estimation," in *Proceedings of the Fourteenth Annual ACM-SIAM Symposium on Discrete Algorithms*. SIAM, Oct. 2020, pp. 378–397.
- [8] J. Chen, M. K. Ng, and D. Wang, "Quantizing heavy-tailed data in statistical estimation:(near) minimax rates, covariate quantization, and uniform recovery," *IEEE Trans. on Inf. Theory*, vol. 70, no. 3, pp. 2003–2038, Mar. 2024.
- [9] J. Chen, Y. Wang, and M. K. Ng, "Quantized low-rank multivariate regression with random dithering," *IEEE Trans. on Signal Process.*, Oct. 2023.
- [10] T. A. Barton and S. T. Smith, "Structured covariance estimation for space-time adaptive processing," in *Proc. IEEE Conf. on Acoust., Speech, and Signal Process.*, vol. 5. IEEE, 1997, pp. 3493–3496.
- [11] J. P. Burg, D. G. Luenberger, and D. L. Wenger, "Estimation of structured covariance matrices," *Proceedings of the IEEE*, vol. 70, no. 9, pp. 963–974, 1982.
- [12] R. A. Roberts and C. T. Mullis, *Digital signal processing*. Addison-Wesley Longman Publishing Co., Inc., 1987.
- [13] A. Gonen, D. Rosenbaum, Y. C. Eldar, and S. Shalev-Shwartz, "Subspace learning with partial information," *Journal of Machine Learning Research*, vol. 17, no. 52, pp. 1–21, Apr. 2016.
- [14] M. I. Miller and D. L. Snyder, "The role of likelihood and entropy in incomplete-data problems: Applications to estimating point-process intensities and toeplitz constrained covariances," *Proc. of the IEEE*, vol. 75, no. 7, pp. 892–907, Jul. 1987.
- [15] T. T. Cai, Z. Ren, and H. H. Zhou, "Optimal rates of convergence for estimating toeplitz covariance matrices," *Probab. Theory and Relat. Fields*, vol. 156, no. 1, pp. 101–143, Mar. 2013.
- [16] Z. Yang, L. Xie, and C. Zhang, "A discretization-free sparse and parametric approach for linear array signal processing," *IEEE Transactions on Signal Processing*, vol. 62, no. 19, pp. 4959–4973, 2014.
- [17] X. Chen, D. M. Kane, E. Price, and Z. Song, "Fourier-sparse interpola-

- tion without a frequency gap,” in *2016 IEEE 57th Annual Symposium on Foundations of Computer Science (FOCS)*. IEEE, 2016, pp. 741–750.
- [18] S. U. Pillai, Y. Bar-Ness, and F. Haber, “A new approach to array geometry for improved spatial spectrum estimation,” *Proc. of the IEEE*, vol. 73, no. 10, pp. 1522–1524, 1985.
- [19] D. Romero, D. D. Ariananda, Z. Tian, and G. Leus, “Compressive covariance sensing: Structure-based compressive sensing beyond sparsity,” *IEEE Signal Process. Mag.*, vol. 33, no. 1, pp. 78–93, Dec. 2015.
- [20] X. Wu, W.-P. Zhu, and J. Yan, “A toeplitz covariance matrix reconstruction approach for direction-of-arrival estimation,” *IEEE Trans. on Veh. Technol.*, vol. 66, no. 9, pp. 8223–8237, Apr. 2017.
- [21] H. Qiao and P. Pal, “Gridless line spectrum estimation and low-rank Toeplitz matrix compression using structured samplers: A regularization-free approach,” *IEEE Trans. on Signal Process.*, vol. 65, no. 9, pp. 2221–2236, May. 2017.
- [22] Z. Yang and K. Wang, “Nonasymptotic performance analysis of direct-augmentation and spatial-smoothing esprit for localization of more sources than sensors using sparse arrays,” *IEEE Transactions on Aerospace and Electronic Systems*, vol. 62, no. 19, pp. 4959–4973, 2023.
- [23] J. Mo and R. W. Heath, “Limited feedback in single and multi-user MIMO systems with finite-bit ADCs,” *IEEE Trans. on Wireless Commun.*, vol. 17, no. 5, pp. 3284–3297, Apr. 2018.
- [24] S. Dirksen, J. Maly, and H. Rauhut, “Covariance estimation under one-bit quantization,” *The Annals of Statistics*, vol. 50, no. 6, pp. 3538–3562, Sep. 2022.
- [25] S. Dirksen and S. Mendelson, “Non-gaussian hyperplane tessellations and robust one-bit compressed sensing,” *J. of the Eur. Math. Soc.*, vol. 23, no. 9, pp. 2913–2947, 2021.
- [26] L. Jacques, J. N. Laska, P. T. Boufounos, and R. G. Baraniuk, “Robust 1-bit compressive sensing via binary stable embeddings of sparse vectors,” *IEEE Trans. on Inf. Theory*, vol. 59, no. 4, pp. 2082–2102, Apr. 2013.
- [27] Y. Plan and R. Vershynin, “One-bit compressed sensing by linear programming,” *Commun. on Pure and Applied Math.*, vol. 66, no. 8, pp. 1275–1297, Sep. 2013.
- [28] L. Jacques and V. Cambareri, “Time for dithering: fast and quantized random embeddings via the restricted isometry property,” *Inf. and Inf.: A Journal of the IMA*, vol. 6, no. 4, pp. 441–476, Apr. 2017.
- [29] H. C. Jung, J. Maly, L. Palzer, and A. Stollenwerk, “Quantized compressed sensing by rectified linear units,” *IEEE Trans. on Inf. Theory*, vol. 67, no. 6, pp. 4125–4149, Nov. 2021.
- [30] R. M. Gray and D. L. Neuhoff, “Quantization,” *IEEE Trans. on Inf. Theory*, vol. 44, no. 6, pp. 2325–2383, Mar. 1998.
- [31] S. Dirksen, “Quantized compressed sensing: a survey,” in *Compressed Sensing and Its Applications: Third International MATHEON Conference 2017*. Springer, 2019, pp. 67–95.
- [32] X. Wu, W.-P. Zhu, and J. Yan, “Direction-of-arrival estimation based on toeplitz covariance matrix reconstruction,” in *Int. Conf. on Acous., Speech and Signal Process. (ICASSP)*. IEEE, 2016, pp. 3071–3075.
- [33] J. Leech, “On the representation of $1, 2, \dots, n$ by differences,” *Journal of the London Mathematical Society*, vol. 1, no. 2, pp. 160–169, 1956.
- [34] N. Shlezinger, M. Chen, Y. C. Eldar, H. V. Poor, and S. Cui, “UVeQFed: Universal vector quantization for federated learning,” *IEEE Trans. on Signal Process.*, vol. 69, pp. 500–514, Jan. 2020.
- [35] H. Zhang, J. Li, K. Kara, D. Alistarh, J. Liu, and C. Zhang, “Zipml: Training linear models with end-to-end low precision, and a little bit of deep learning,” in *Int. Conf. on Machine Learning*. PMLR, 2017, pp. 4035–4043.
- [36] J. Chen, C.-L. Wang, M. K. Ng, and D. Wang, “High dimensional statistical estimation under uniformly dithered one-bit quantization,” *IEEE Trans. on Inf. Theory*, vol. 69, no. 8, pp. 5151–5187, Jan. 2023.
- [37] R. M. Gray and T. G. Stockham, “Dithered quantizers,” *IEEE Trans. on Inf. Theory*, vol. 39, no. 3, pp. 805–812, May. 1993.
- [38] M. Meckes, “On the spectral norm of a random Toeplitz matrix,” *Electronic Communications in Probability*, vol. 12, no. none, pp. 315 – 325, 2007.
- [39] S. Negahban and M. J. Wainwright, “Estimation of (near) low-rank matrices with noise and high-dimensional scaling,” *The Annals of Statistics*, vol. 39, no. 2, pp. 1069 – 1097, 2011.
- [40] R. M. Gray *et al.*, “Toeplitz and circulant matrices: A review,” *Foundations and Trends® in Communications and Information Theory*, vol. 2, no. 3, pp. 155–239, 2006.
- [41] Z. Yang, L. Xie, and P. Stoica, “Vandermonde decomposition of multilevel toeplitz matrices with application to multidimensional super-resolution,” *IEEE Transactions on Information Theory*, vol. 62, no. 6, pp. 3685–3701, 2016.
- [42] R. Vershynin, *High-dimensional probability: An introduction with applications in data science*. Cambridge university press, 2018, vol. 47.